Long-Term Thermal Stability of High-Efficiency Polymer Solar Cells Based on Photocrosslinkable Donor-Acceptor Conjugated Polymers

Gianmarco Griffini, Jessica D. Douglas, Claudia Piliego, Thomas W. Holcombe, Stefano Turri, Jean M. J. Fréchet, and Justin L. Mynar**

Solution-processable polymer-based organic photovoltaics (OPVs) have attracted considerable attention over the past two decades because of the many advantages they can provide: low-cost fabrication, flexible devices, and light-weight construction.[1] In the most successful OPV device architectures, the photoactive layer is composed of a blend of a p-type conjugated polymer and an n-type fullerene derivative, forming the so-called donor–acceptor bulk heterojunction (BHJ).[2]

Recently, the long-term stability of OPV devices has been recognized as an important area of research, both in academia and industry.[3] Concerning this issue, a number of studies have demonstrated the detrimental effects of oxygen and moisture on device operation,[4] and attempts have been made to elucidate the degradation mechanism of the photoactive organic layer.[5] In addition to chemical degradation pathways, achieving and maintaining an effective BHJ morphology within the active layer is critical for sustaining high OPV performance. In optimized BHJs, phase separation of the electron donor and the electron acceptor domains should be on the same length-scale as the exciton diffusion length, facilitating efficient exciton harvesting.[6] Furthermore, a 3D bicontinuous network of the donor and acceptor materials is necessary for productive charge extraction from the device.[7]

Although an optimized BHJ morphology can be attained by means of several processing techniques,[8] the peak-performance morphology only represents a metastable state, which cannot usually be maintained over long operation times. In fact, most BHJ systems show poor stability and often undergo macrophase segregation of the blend components, especially after prolonged exposure to heat.[9] Considering that normal OPV device operation may subject the active layer to large temperature fluctuations, improving the robustness of the BHJ with respect to thermal stability is critical.[10]

Several studies have reported on the morphological evolution and thermal stability of the active layer in standard BHJ systems such as blends of poly(3-hexylthiophene) (P3HT):[6,6]-phenyl-C_{61}-butyric acid methyl ester ($PC_{61}BM$) or poly[2-methoxy-5-(3',7'-dimethyloctyloxy)-1,4-phenylenevinylene] (MDMO-PPV):$PC_{61}BM$. In such systems, phase segregation in the active layer occurs upon thermal annealing, resulting first in an improvement followed by a quick decline in device performance, particularly at high temperatures.[11–13] In order to improve the thermal stability of these OPV devices, different strategies have been presented, which include the use of diblock copolymer compatibilizers,[14] the use of fullerene-attached diblock copolymers,[15] and the use of both thermally crosslinkable acceptor[16] and donor[17] materials within the active layer. Recently, our group synthesized a library of photocrosslinkable P3HT copolymers containing some light-sensitive bromoalkyl substituents for use as p-type materials in BHJ devices. Utilizing these materials, it was shown that even after two days of annealing at an elevated temperature of 150 °C, the devices containing the photocrosslinked polymer within the active layer were able to retain their initial power conversion efficiency (PCE). This result was attributed to the stabilizing effect of the photocrosslinked polymer on the nanoscale morphology of the active layer.[18] In contrast to thermal crosslinking, photocrosslinking does not interfere with the thermal treatments that are often needed during device optimization; thus, this process allows for morphology optimization with independent control of crosslinking and thermal annealing.

Although BHJ devices based on the P3HT:$PC_{61}BM$ blend represent a benchmark in the OPV literature, new p-type polymers have been synthesized in an effort to improve device efficiencies.[19] In particular, the copolymerization of electron-rich and electron-poor monomers, constituting the so-called donor–acceptor (D–A) approach, has proven to be an effective strategy to obtain low-bandgap polymers with optical and electronic properties that can be tuned via synthetic control of the electron-rich and electron-poor units. Using this strategy, reports have demonstrated PCEs approaching 7–8%, after systematic optimization of appropriate device parameters.[20] However, the thermal stability of OPVs based on D–A polymers has yet to be investigated in detail: no example of long-term thermally stable devices based on this class of high-efficiency p-type polymers has been reported to date.

G. Griffini, J. D. Douglas, Dr. C. Piliego, T. W. Holcombe, Prof. J. M. J. Fréchet, Dr. J. L. Mynar
Departments of Chemistry and Chemical Engineering
University of California
Berkeley, Berkeley, CA 94720-1460, USA
E-mail: frechet@berkeley.edu; jmynar@gmail.com
G. Griffini, J. D. Douglas, Dr. C. Piliego, T. W. Holcombe, Prof. J. M. J. Fréchet, Dr. J. L. Mynar
Materials Science Division
Lawrence Berkeley National Laboratory
Berkeley, CA 94720, USA
G. Griffini, Prof. S. Turri
Department of Chemistry
Materials and Chemical Engineering "Giulio Natta"
Politecnico di Milano, Piazza Leonardo da Vinci 32, 20133 Milan, Italy

DOI: 10.1002/adma.201004743

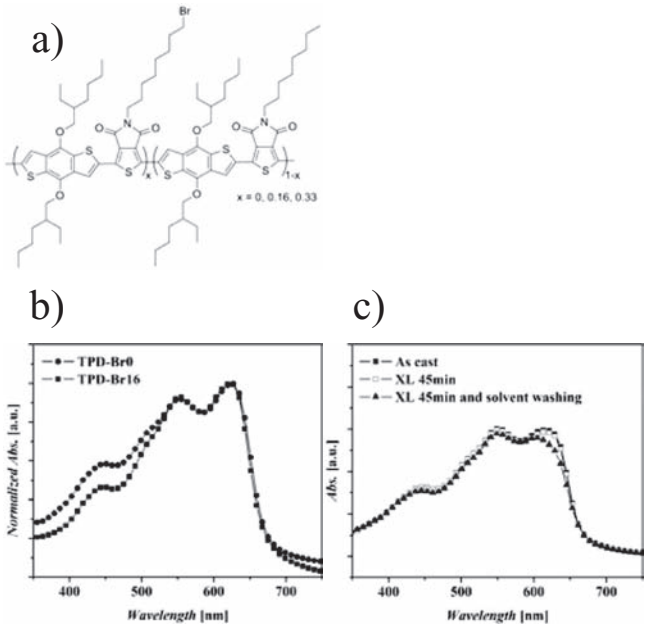

Figure 1. a) Molecular structure of the polymers used in this study. b) Normalized absorption spectra of polymer films without Br substituents (TPD-Br0) and with 16% Br substituents (TPD-Br16) in the polymer chain. c) Absorption spectra of TPD-Br16 polymer films pristine (as cast), after 45 min of UV-irradiation (photocrosslinking (XL) 45 min), and after UV-irradiation and solvent washing (XL 45 min and solvent washing).

Herein, we report the first study on the thermal stability of OPV devices based on D–A copolymers. Through a new synthetic pathway, we have developed a photocrosslinkable derivative of the thieno[3,4-*c*]pyrrole-4,6-dione (TPD)-based polymer that was recently reported.[20c,e] The new polymer contains TPD repeat units with a terminal, primary bromide functionality appended to the octyl solubilizing group (TPD-Br) (see **Figure 1**a), thereby allowing for photocrosslinking of the polymer in devices. By synthetically tuning the number of Br units in the polymer and by employing UV-mediated photocrosslinking, OPV devices with high PCE and excellent thermal stability were fabricated. Devices employing copolymers with varying amounts of Br units were tested: 0% Br-units (TPD-Br0), 16% Br-units (TPD-Br16), and 33% Br-units (TPD-Br33). The best OPV performance after annealing was obtained with photocrosslinked TPD-Br16. In contrast to the sharp PCE decrease observed for TPD-Br0 devices, the annealed OPVs based on photocrosslinked TPD-Br16 demonstrated remarkable long-term thermal stability. After 72 h of thermal annealing at 150 °C, an average PCE of 4.6% ± 0.1% was obtained with a short circuit current density (J_{SC}) of 10.1 mA cm^{-2}, an open circuit voltage (V_{OC}) of 0.85 V, and a fill factor (*FF*) of 54%. The maximum PCE obtained was as high as 4.7%. To the best of our knowledge, this represents the highest PCE reported thus far, for OPV systems subjected to long-term thermal annealing at high temperature.

The normalized UV-vis absorption spectra of the as-cast TPD-Br16 and TPD-Br0 polymers are shown in Figure 1b. Both polymers exhibit three maxima between 400 nm and 700 nm, in accordance with previous reports.[20c,e] Furthermore, no major differences can be observed between the absorption spectra of the two polymers, indicating that the addition of Br units to the polymer does not significantly affect its optical properties. Figure 1c shows the UV-vis absorption spectra of TPD-Br16 films as-cast and after photocrosslinking. After 45 min of UV irradiation, the polymer film becomes resistant to solvent washing. With thermal annealing, no solvent resistance is observed.[18] The absorption intensity at 550 nm after UV-irradiation and washing with solvent differs by less than 4% from the absorption intensity of the as-cast film, indicating that photocrosslinking has occurred. In addition, no major differences in the absorption spectra of as-cast and photocrosslinked films are observed, indicating that the photocrosslinking process does not significantly affect the optical properties of the solid state polymer. A similar trend was observed for the TPD-Br33 film (see Supporting Information). On the other hand, TPD-Br0 polymer containing no Br units does not undergo photocrosslinking when irradiated with UV light as evidenced by low resistance to solvent washing.

The performance of the corresponding OPV devices was investigated using the indium tin oxide (ITO)/poly(3,4-ethylenedioxythiophene) (PEDOT):poly(styrenesulfonate) (PSS)/polymer:[6,6]-phenyl-C_{71}-butyric acid methyl ester ($PC_{71}BM$)/Ca/Al device architecture. After optimization of TPD-Br16 and TPD-Br33 device parameters, *ortho*-dichlorobenzene (*o*-DCB) was chosen as the solvent for the active layer blend deposition. In addition, these devices do not contain high-boiling-point solvent additives,[21] as they did not yield any improvement to the performance of the TPD-Br16 and TPD-Br33 OPV devices. $PC_{71}BM$ was employed as the n-type material because it was found to yield higher device performance compared to $PC_{61}BM$ during device optimization (see Supporting Information).

The thermal stability of TPD-Br16 devices is shown in **Figure 2**a, where the performances of both photocrosslinked (TPD-Br16 XL) and non-photocrosslinked (TPD-Br16 no XL) devices are shown. For comparison, the thermal stability of TPD-Br0 devices is also shown. The average device parameters at 0 h and 72 h annealing are listed in **Table 1**. An optimal polymer:$PC_{71}BM$ wt.-ratio of 1:2 was found for both TPD-Br0 and TPD-Br16 polymer systems (see Supporting Information for details on device fabrication). The initial performance of TPD-Br16 no XL devices (5.6% PCE) is comparable to that of TPD-Br0 devices (5.2% PCE), suggesting that the introduction of a terminal alkyl-bromine functionality on the solubilizing group of TPD does not detrimentally affect the optical properties of the polymer and the PV performance of the OPV devices at this incorporation ratio. On the other hand, TPD-Br16 XL devices show a significantly lower initial PCE (3.3%) with respect to both TPD-Br0 and TPD-Br16 no XL. This can be attributed to the effect of crosslinking on the π-stacking of the polymer chains, affecting the electronic properties of the polymer and the OPV device performance.[20c] However, a striking difference is observed between TPD-Br16 XL and the other two devices upon exposure to heat: while both TPD-Br0 and TPD-Br16 no XL devices undergo a sharp decrease in performance upon thermal annealing over time, TPD-Br16 XL devices show an increase in PCE, which stabilizes after 24 h of annealing. A PCE as high as 4.6% was obtained for the crosslinked polymer after 72 h of annealing at 150 °C. This

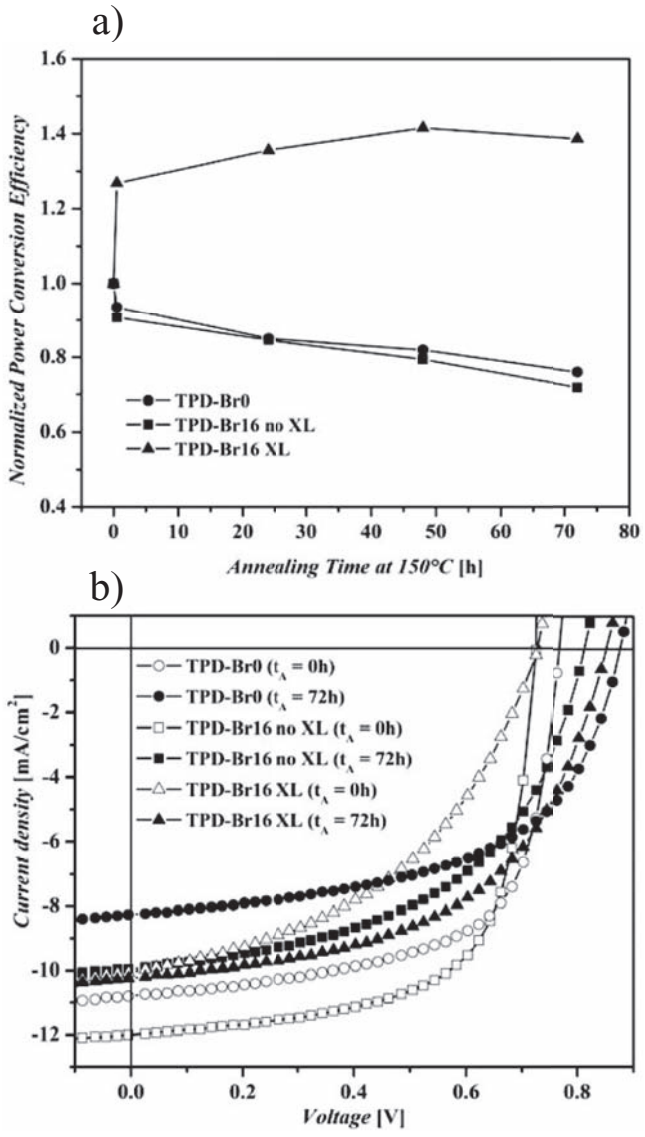

Figure 2. a) Normalized PCEs of TPD-Br0 (●), non-photocrosslinked TPD-Br16 (no XL ■), and photocrosslinked TPD-Br16 (XL ▲) devices during long-term thermal annealing at 150 °C with $PC_{71}BM$ as n-type material. The efficiency of each device was normalized to its initial efficiency (at annealing time 0 h). The same blend concentration (24 mg mL^{-1} in dichlorobenzene) and polymer:$PC_{71}BM$ ratio (1:2) was used for all devices. b) Current–voltage (*J*–*V*) curves of the best OPV devices before (open symbols, t_A = 0 h) and after (full symbols, t_A = 72 h) long-term thermal annealing (t_A).

represents the first demonstration of long-term thermally stable OPV devices based on a D–A polymer.

The evolution of device performance with annealing time for the three systems reported in Figure 2a can be better understood by analyzing the *J*–*V* output characteristics recorded at annealing times 0 h and 72 h at 150 °C (see Figure 2b). An increase in the V_{OC} is observed for all devices after 72 h of annealing at high temperature. This increase may be related to a change in the energy of the interfacial charge-transfer states between the polymer and fullerene caused by morphological

Table 1. Characteristic photovoltaic parameters for TPD-Br0:$PC_{71}BM$ and TPD-Br16:$PC_{71}BM$ devices.

	XL[a)]	Annealing time t_A [h]	J_{SC} [mA cm^{-2}]	V_{OC} [V]	*FF* [%]	PCE (PCE_{max}) [%]
TPD-Br0	–	0	–10.6	0.76	64	5.2 (5.3)
TPD-Br0	–	72	–8.2	0.87	55	3.9 (4.1)
TPD-Br16	–	0	–11.7	0.73	66	5.6 (5.7)
TPD-Br16	–	72	–9.6	0.81	51	4.0 (4.2)
TPD-Br16	+	0	–10.0	0.73	45	3.3 (3.3)
TPD-Br16	+	72	–10.1	0.85	53	4.6 (4.7)

[a)]Active layers not subjected (–) and subjected (+) to crosslinking under UV irradiation prior to cathode deposition.

rearrangement of the fullerene molecules adjacent to the polymer chains after annealing.[22] However, both TPD-Br0 and TPD-Br16 no XL devices undergo a significant decrease in their short-circuit current density and fill factor during annealing, which results in a sharp decrease in PCE with respect to the initial values. Conversely, the J_{SC} of TPD-Br16 XL devices remains constant, even after 72 h of annealing at 150 °C, while the fill factor increases about 18% compared to its initial value. This indicates that photocrosslinking has allowed for an optimal morphology of the active layer to be preserved throughout the entire annealing process, thus leading to remarkable long-term thermal stability of these devices. Similar trends were found for TPD-Br33 devices, although lower PCEs with respect to TPD-Br16 were observed for both the non-photocrosslinked and the photocrosslinked systems (see Supporting Information). This indicates that judicious control of the TPD-Br content in the polymer is necessary to ensure optimal PV performances.

In order to clarify the effect of photocrosslinking on the morphology of the active layer, atomic force microscopy (AFM) was performed on both TPD-Br16 no XL and TPD-Br16 XL films (see **Figure 3**). Before thermal annealing, the non-photocrosslinked TPD-Br16 active layer film (Figure 3a,b) shows a well-developed interpenetrating network and a finer nanoscale morphology compared to the photocrosslinked film (Figure 3e,f). The surface root-mean-square (RMS) roughness before annealing is 2.5 nm and 2.1 nm for non-photocrosslinked and photocrosslinked films, respectively. After annealing at 150 °C for 72 h, a very rough surface morphology is observed on the non-photocrosslinked film (Figure 3c,d), resulting in a value of RMS roughness as high as 34.9 nm. This significant morphology change may yield poor contact between the active layer and the electrode, as well as unfavorable conditions for charge separation and transport. Accordingly, a significant decrease in device performance is observed for the TPD-Br16 no XL device after annealing. On the other hand, a finer morphology is observed for the photocrosslinked film after annealing (Figure 3g,h), which is correlated to the increase in device PCE. Only a slight increase in RMS roughness is observed for this film (up to 3.0 nm), suggesting that photocrosslinking allows for the preservation of a well-developed interpenetrating donor/acceptor network that can be maintained, even after 72 h of annealing at 150 °C.

It is worth mentioning that during device optimization, each polymer was also tested in BHJ devices with $PC_{61}BM$

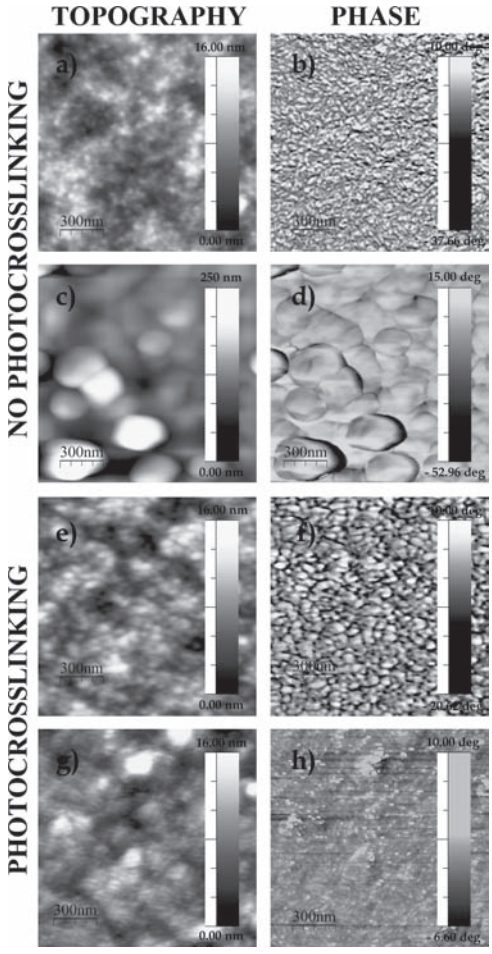

Figure 3. AFM (1.5 μm × 1.5 μm) topography and phase images of TPD-Br16:$PC_{71}BM$ active layers (1:2 wt:wt). The top four images are for the non-crosslinked films (TPD-Br16 no XL), prior to (a,b) and after (c,d) 72 h of thermal annealing at 150 °C. The bottom four images are for the crosslinked devices (TPD-Br16 XL), prior to (e,f) and after (g,h) 72 h of thermal annealing at 150 °C.

(see Supporting Information). As opposed to BHJs containing photocrosslinked polymer and $PC_{71}BM$, devices containing photocrosslinked polymer and $PC_{61}BM$ showed a peak PCE after 30 min of annealing at 150 °C that was not maintained after longer annealing times. Additionally, AFM analysis revealed the formation of aggregates in both photocrosslinked and non-photocrosslinked active layers after 72 h of annealing at 150 °C, although a rougher surface was found for non-photocrosslinked films (see Supporting Information). We speculate that the different behavior found for polymer:$PC_{61}BM$ blends compared to polymer:$PC_{71}BM$ blends may be related to the different sizes of these fullerene molecules (1.67 vs 1.92 nm)[23] and their movement during the annealing process. Thermal annealing appears to allow the smaller $PC_{61}BM$ molecules to diffuse within the crosslinked polymer network, initially improving the performance but ultimately leading to formation of larger aggregates, whereas this effect is not observed with $PC_{71}BM$. Due to steric bulkiness, the larger $PC_{71}BM$ molecules may be confined into the polymer network, thus inhibiting the formation of large aggregates. This result may indicate that, in addition to increased light absorption with respect to $PC_{61}BM$, $PC_{71}BM$ is able to provide morphological stability of the active layer at high temperature. Further investigations to clarify these observations are underway.

In summary, the first photocrosslinkable donor–acceptor conjugated polymer for use in BHJ organic solar cells was developed. After 72 h of thermal annealing at 150 °C, a stable PCE of 4.6% was obtained in devices containing photocrosslinked polymer in the active layer. This represents the highest performance reported thus far for thermally stable OPV devices. Careful control of the crosslinking moiety content in the polymer was found to be critical in order to achieve optimal device performance. The results of this study provide important guidelines for the design and development of OPV materials with long-term thermal stability and high efficiency.

Supporting Information

Supporting Information is available from the Wiley Online Library or from the author.

Acknowledgements

This work is part of the "Plastics Electronics" program at Lawrence Berkeley National Laboratory and was supported by the Director, Office of Science, Office of Basic Energy Sciences, Materials Sciences and Engineering Division, of the U.S. Department of Energy under Contract No. DE-AC02-05CH11231 (all experimental work). G.G. thanks Fondazione Banca del Monte di Lombardia; T.W.H. thanks the National Science Foundation, and J.D.D. thanks the Natural Sciences and Engineering Research Council of Canada for research fellowships. The authors thank Dr. Jill Millstone and Claire Woo for helpful discussions.

Received: December 27, 2010
Published online: February 22, 2011

[1] a) C. J. Brabec, S. Gowrisanker, J. J. M. Halls, D. Laird, S. Jia, S. P. Williams, *Adv. Mater.* **2010**, *22*, 3839; b) G. Dennler, M. C. Scharber, C. J. Brabec, *Adv. Mater.* **2009**, *21*, 1323; c) B. Kippelen, J. L. Brédas, *Energy Environ. Sci.* **2009**, *2*, 251; d) B. C. Thompson, J. M. J. Fréchet, *Angew. Chem. Int. Ed.* **2008**, *47*, 58; e) F. C. Krebs, J. Fyenbo, M. Jørgensen, *J. Mater. Chem.* **2010**, *20*, 8994; f) F. C. Krebs, T. D. Nielsen, J. Fyenbo, M. Wadstrøm, M. S. Pedersen, *Energy Environ. Sci.* **2010**, *3*, 512.

[2] a) G. Yu, J. Gao, J. C. Hummelen, F. Wudl, A. J. Heeger, *Science* **1995**, *270*, 1789; b) G. Yu, A. J. Heeger, *J. Appl. Phys.* **1995**, *78*, 4510.

[3] M. Jørgensen, K. Norrman, F. C. Krebs, *Sol. Energy Mater. Sol. Cells* **2008**, *92*, 686.

[4] a) F. C. Krebs, H. Spanggaard, *Chem. Mater.* **2005**, *17*, 5235; b) F. C. Krebs, K. Norrman, *Prog. Photovoltaics* **2007**, *15*, 697; c) M. O. Reese, A. J. Morfa, M. S. White, N. Kopidakis, S. E. Shaheen, G. Rumbles, D. S. Ginley, *Sol. Energy Mater. Sol. Cells* **2008**, *92*, 746; d) A. Seemann, H. J. Egelhaaf, C. J. Brabec, J. A. Hauch, *Org. Electron.* **2009**, *10*, 1424.

[5] a) M. Manceau, S. Chambon, A. Rivaton, J. L. Gardette, S. Guillerez, N. Lemaitre, *Sol. Energy Mater. Sol. Cells* **2010**, *94*, 1572; b) M. O. Reese, A. M. Nardes, B. L. Rupert, R. E. Larsen, D. C. Olson, M. T. Lloyd, S. E. Shaheen, D. S. Ginley, G. Rumbles, N. Kopidakis,

Adv. Funct. Mater. **2010**, *20*, 3476.; c) A. Rivaton, S. Chambon, M. Manceau, J. L. Gardette, N. Lamaitre, S. Guillerez, *Polym. Degrad. Stab.* **2010**, *95*, 278.
[6] S. K. Pal, T. Kesti, M. Maiti, F. Zhang, O. Inganäs, S. Hellström, M. R. Andersson, F. Oswald, F. Langa, T. Österman, T. Pascher, A. Yartsev, V. Sundström, *J. Am. Chem. Soc.* **2010**, *132*, 12440.
[7] a) W. L. Ma, C. Y. Yang, X. Gong, K. Lee, A. J. Heeger, *Adv. Funct. Mater.* **2005**, *15*, 1617; b) X. Yang, J. Loos, *Macromolecules* **2007**, *40*, 1353.
[8] J. Peet, M. L. Senatore, A. J. Heeger, G. C. Bazan, *Adv. Mater.* **2009**, *21*, 1521.
[9] a) S. Bertho, G. Janssen, T. J. Cleij, B. Conings, W. Moons, A. Gadisa, J. D'Haen, E. Goovaerts, L. Lutsen, J. Manca, D. Vanderzande, *Sol. Energy Mater. Sol. Cells* **2008**, *92*, 753; b) B. Paci, A. Generosi, V. Rossi Albertini, R. Generosi, P. Perfetti, R. de Bettignies, C. Sentein, *J. Phys. Chem. C* **2008**, *112*, 9931.
[10] a) D. Di Nuzzo, A. Aguirre, M. Shahid, V. S. Gevaerts, S. C. J. Meskers, R. A. J. Janssen, *Adv. Mater.* **2010**, *22*, 4321; b) M. Helgesen, M. Bjerring, N. C. Nielsen, F. C. Krebs, *Chem. Mater.* **2010**, **22**, 5617.
[11] B. Conings, S. Bertho, K. Vandewal, A. Senes, J. D'Haen, J. Manca, R. A. J. Janssen, *Appl. Phys. Lett.* **2010**, *96*, 163301.
[12] a) X. N. Yang, J. Loos, S. C. Veenstra, W. J. H. Verhees, M. M. Wienk, J. M. Kroon, M. A. J. Michels, R. A. J. Janssen, *Nano Lett.* **2005**, *5*, 579; b) X. N. Yang, J. K. J. van Duren, R. A. J. Janssen, M. A. J. Michels, J. Loos, *Macromolecules* **2004**, *37*, 2151.
[13] K. Sivula, C. K. Luscombe, B. C. Thompson, J. M. J. Fréchet, *J. Am. Chem. Soc.* **2006**, *128*, 13988.
[14] K. Sivula, Z. T. Ball, N. Watanabe, J. M. J. Fréchet, *Adv. Mater.* **2006**, *18*, 206.
[15] S. Miyanishi, Y. Zhang, K. Tajima, K. Hashimoto, *Chem. Commun.* **2010**, *46*, 6723.
[16] M. Drees, H. Hoppe, C. Winder, H. Neugebauer, N. S. Sariciftci, W. Schwinger, F. Schaffler, C. Topf, M. C. Scharber, Z. G. Zhu, R. Gaudiana, *J. Mater. Chem.* **2005**, *15*, 5158.
[17] S. Miyanishi, K. Tajima, K. Hashimoto, *Macromolecules* **2009**, *42*, 1610.
[18] B. J. Kim, Y. Miyamoto, B. W. Ma, J. M. J. Fréchet, *Adv. Funct. Mater.* **2009**, *19*, 2273.
[19] a) E. Bundgaard, F. C. Krebs, *Sol. Energy Mater. Sol. Cells* **2007**, *91*, 954; b) H. Y. Chen, J. H. Hou, S. Q. Zhang, Y. Y. Liang, G. W. Yang, Y. Yang, L. P. Yu, Y. Wu, G. Li, *Nat. Photonics* **2009**, *3*, 649; c) Y. F. Li, Y. P. Zou, *Adv. Mater.* **2008**, *20*, 2952.
[20] a) L. J. Huo, J. H. Hou, S. Q. Zhang, H. Y. Chen, Y. Yang, *Angew. Chem. Int. Ed.* **2010**, *49*, 1500; b) Y. Y. Liang, Z. Xu, J. B. Xia, S. T. Tsai, Y. Wu, G. Li, C. Ray, L. P. Yu, *Adv. Mater.* **2010**, *22*, E135; c) C. Piliego, T. W. Holcombe, J. D. Douglas, C. H. Woo, P. M. Beaujuge, J. M. J. Fréchet, *J. Am. Chem. Soc.* **2010**, *132*, 7595; d) Y. Zhang, S. K. Hau, H. L. Yip, Y. Sun, O. Acton, A. K. Y. Jen, *Chem. Mater.* **2010**, *22*, 2696; e) Y. P. Zou, A. Najari, P. Berrouard, S. Beaupre, B. R. Aich, Y. Tao, M. Leclerc, *J. Am. Chem. Soc.* **2010**, *132*, 5330.
[21] a) C. V. Hoven, X. D. Dang, R. C. Coffin, J. Peet, T. Q. Nguyen, G. C. Bazan, *Adv. Mater.* **2010**, *22*, E63; b) J. K. Lee, W. L. Ma, C. J. Brabec, J. Yuen, J. S. Moon, J. Y. Kim, K. Lee, G. C. Bazan, A. J. Heeger, *J. Am. Chem. Soc.* **2008**, *130*, 3619.
[22] a) K. Vandewal, K. Tvingsted, A. Gadisa, O. Inganäs, J. V. Manca, *Phys. Rev. B* **2010**, *81*, 125204; b) M. D. Perez, C. Borek, S. R. Forrest, M. E. Thompson, *J. Am. Chem. Soc.* **2009**, *131*, 9281.
[23] T. Kawauchi, J. Kumaki, A. Kitaura, K. Okoshi, H. Kusanagi, K. Kobayashi, T. Sugai, H. Shinohara, E. Yashima, *Angew. Chem. Int. Ed.* **2008**, *47*, 515.